Inorganic Chemistry

Article

pubs.acs.org/IC

A Ferromagnetic Methoxido-Bridged Mn(III) Dimer and a Spin-Canted Metamagnetic $\mu_{1,3}$-Azido-Bridged Chain

Subrata Naiya,[†,‡] Saptarshi Biswas,[†] Michael G. B. Drew,[§] Carlos J. Gómez-García,*[,∥] and Ashutosh Ghosh*[,†]

[†]Department of Chemistry, University College of Science, University of Calcutta, 92, APC Road, Kolkata 700 009, India

[‡]Susil Kar College, Ghoshpur, Champahati, Baruipur, 24 Parganas(S), West Bengal 743 330, India

[§]School of Chemistry, The University of Reading, P.O. Box 224, Whiteknights, Reading RG 66AD, United Kingdom

[∥]Instituto de Ciencia Molecular (ICMol), Parque Científico, Universidad de Valencia, C/Catedrático José Beltrán, 2. 46980 Paterna, Valencia, Spain

Supporting Information

ABSTRACT: Two new Mn(III) complexes of formulas $[MnL^1(N_3)(OMe)]_2$ (**1**) and $[MnL^2(N_3)_2]_n$ (**2**) have been synthesized by using two tridentate NNO-donor Schiff base ligands HL^1 {(2-[(3-methylaminoethylimino)-methyl]-phenol)} and HL^2 {(2-[1-(2-dimethylaminoethylimino)methyl]-phenol)}, respectively. Substitution of the H atom on the secondary amine group of the N-methyldiamine fragment of the Schiff base by a methyl group leads to a drastic structural change from a methoxido-bridged dimer (**1**) to a single $\mu_{1,3}$-azido-bridged 1D helical polymer (**2**). Both complexes were characterized by single-crystal X-ray structural analyses and variable-temperature magnetic susceptibility measurements. The magnetic properties of compound **1** show the presence of weak ferromagnetic exchange interactions mediated by double methoxido bridges (J = 0.95 cm^{-1}). Compound **2** shows the existence of a weak antiferromangetic coupling along the chain (J = −8.5 cm^{-1}) through the single $\mu_{1,3}$-N_3 bridge with a spin canting that leads to a long-range antiferromagnetic order at $T_c \approx 9.3$ K and a canting leading to a weak ferromagnetic long-range order at $T_c \approx 8.5$ K. It also exibits metamagnetic behavior at low temperatures with a critical field of ca.1.2 T due to the weak antiferromagnetic interchain interactions that appear in the canted ordered phase.

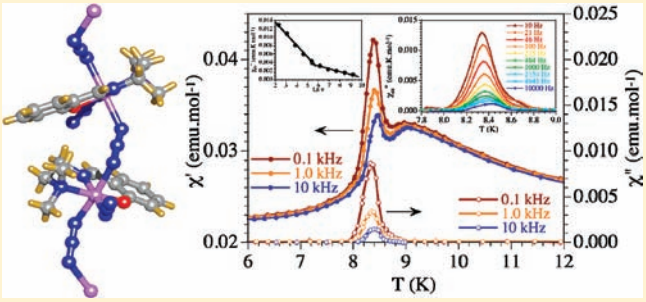

INTRODUCTION

The study of magnetically ordered molecule-based materials and their structure−function relationships is a very fast growing area in chemistry. Among these materials, one of the most widely investigated systems is the ferromagnetically coupled polynuclear clusters of transition metal ions that behave like magnets, i.e., single-molecule magnets (SMMs).[1,2] The compounds containing high-spin Mn(III) are often found to behave like SMMs[2a,c,d] because the Mn(III) ion possesses a large spin value (S = 2)[2,3] and a pronounced single ion easy axis anisotropy induced by Jahn−Teller elongation of the coordination octahedron. However, ferromagnetic interactions that would result in a high-spin ground state of the cluster are by far less common than the antiferromagnetic ones.[4] A recent development in magnetism of 1D chain compounds reveals that antiferromagnetic interactions between similar spins in principle can also give rise to a magnetic behavior like SMMs, provided that magnetic anisotropy is present and the easy axes are not collinear.[1,2] In such a case, the angle between the AF-coupled moments is not exactly 180°, resulting in an uncompensated small moment per magnetic center. These small moments are all aligned in the same direction (almost perpendicular to the original local moments) and generate a ferromagnetic arrangement of small moments (weak ferromangetism) that may give rise to canted single chain magnets (SCMs).[1e,5]

Besides the spin carrier, the judicious choice of bridging atoms or groups is also crucial to the design of new molecular magnets. Usually, ligands containing one to three atoms are very efficient in transmitting the magnetic coupling. The azide ion is such a ligand that has been used extensively for the construction of various magnetic systems[6,7] for its versatile bridging modes (Scheme 1). Moreover, the nature of the magnetic coupling between the metal centers is exceedingly dependent on the bridging modes of azide.[6−9] Usually, the $\mu_{1,1}$ bridging mode transmits ferromagnetic,[6a,10] and the $\mu_{1,3}$ bridging mode transmits antiferromagneic couplings.[6a,7c,11] Consequently, numerous azido-bridged compounds of Cu(II), Ni(II), and Mn(II) having different types of magnetic behavior, e.g., ferromagnetic,[6a,10] antiferromagnetic,[6a,7c,11] metamagnetic,[12] spin-canting,[4b,12,13] spin flop,[14] etc. have been reported.

Received: February 6, 2012
Published: April 11, 2012

   dx.doi.org/10.1021/ic300274n | *Inorg. Chem.* 2012, 51, 5332−5341

Scheme 1. Various Azido Bridging Modes

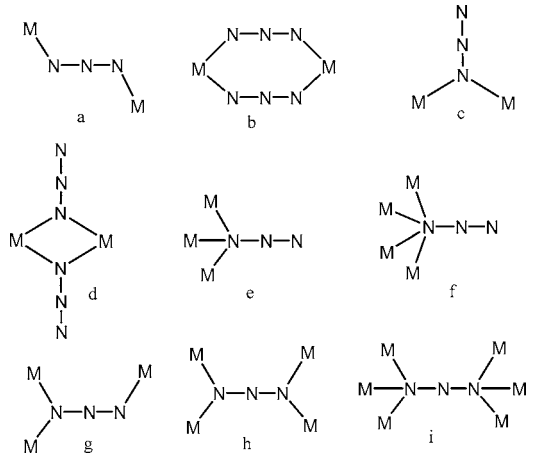

Scheme 2. Synthetic Routes of the Complexes

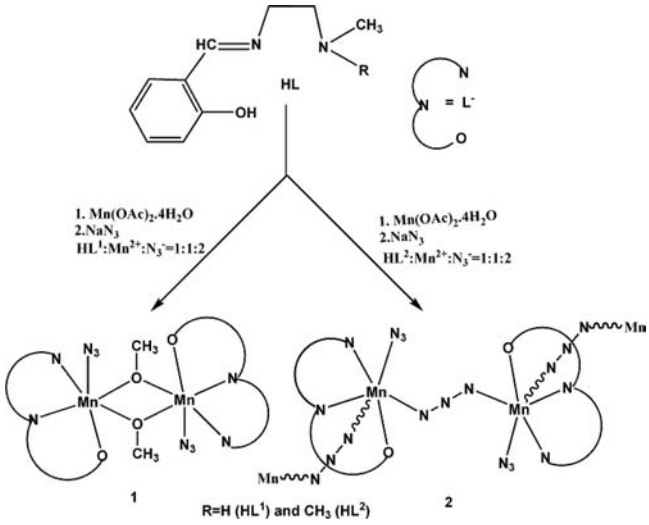

Azido-bridged complexes containing only Mn(III) are less common, although a careful search in the CCDC database (updated November 2011) shows that there are 12 discrete complexes (with nuclearities from 2 to 13) with μ-N_3 bridges: seven with $\mu_{1,1}$-N_3 (Scheme 1c),[15] three with $\mu_{1,3}$-N_3 (Scheme 1a),[16] one with both $\mu_{1,1}$-N_3 and $\mu_{1,3}$-N_3 bridges[17] and one with $\mu_{1,1,1}$-N_3 bridges (Scheme 1a),[18] five chains formed by oxido-centered Mn_3O building units connected through $\mu_{1,3}$-N_3 bridges,[19] 12 Mn(III) chains (11 with $\mu_{1,3}$-N_3 bridges[20] and one with $\mu_{1,1}$-N_3 bridges),[21] and only one 3D compound.[22] Most of these compounds (ca. 2/3) have been prepared with Schiff-base ligands since, on reacting with such ligands, Mn(II) can readily be oxidized in the air to Mn(III) and stabilized by complex formation. Most of these Schiff-base ligands are tetradentate N_2O_2 or tridentate NO_2 donors, but none present a tridentate N_2O donor set, as observed in our compound **2**, even though such tridentate N_2O Schiff-base ligands are very common in Cu(II) and Ni(II) systems for the construction of polynuclear complexes with interesting structures and magnetic properties.[6a,10b,23]

Here, we report the synthesis, crystal structure, and magnetic properties of two Mn(III) complexes $[MnL^1(N_3)(OMe)]_2$ (**1**) and $[MnL^2(N_3)_2]_n$ (**2**) with the Schiff-base ligands HL^1 = (2-[(3-methylaminoethylimino)-methyl]-phenol) and HL^2 = (2-[1-(2-dimethylaminoethylimino)methyl]phenol) (Scheme 2). In compound **1**, the Mn(III) ions are ferromagnetically coupled via a double methoxido bridge. Compound **2** is a Mn(III) chain with single $\mu_{1,3}$-N_3 bridges that presents an antiferromagnetic coupling with a long-range canted antiferromagnetic ordering and metamagnetic behavior at low temperatures.

EXPERIMENTAL SECTION

Materials. The two tridentate Schiff base ligands, HL^1 and HL^2, have been synthesized in our laboratory according to the methods described below. The diamines and salicyldehyde were purchased from Lancaster Chemical Co. The chemicals were of reagent grade and used without further purification.

Caution! *Although no incidents were recorded in this study, azido salts of metal complexes with organic ligands are potentially explosive. Only a small amount of material should be prepared, and it should be handled with care.*

The ligands HL^1 and HL^2 were prepared by refluxing salicylaldehyde (0.5 mL, 5 mmol) with N-methylethane-1,2-diamine (0.3 mL, 5 mmol) and N,N-dimethylethane-1,2-diamine (0.55 mL, 5 mmol), respectively, in methanol (30 mL) for 30 minutes. The resulting dark yellow solutions of the tridentate ligands HL^1 and HL^2 were subsequently used for complex formation.

*Synthesis of $[MnL^1(N_3)(OMe)]_2$ (**1**).* At room temperature, 5 mmol of methanolic solution of Schiff base ligand HL^1 (10 mL) was added to a 20 mL methanolic solution of $Mn(OAc)_2{\cdot}4H_2O$ (1.225 g, 5 mmol) followed by an aqueous solution (5 mL) of NaN_3 (0.650 g, 10 mmol). The solution turned red. The mixture was kept unstirred in a refrigerator. The red colored, X-ray quality, prismatic shaped single crystals started to separate within a few hours and were collected after 2 days.

Complex **1**. Yield: 0.950 g. (74%). $C_{22}H_{32}Mn_2N_{10}O_4$ (610.44) calcd.: C, 43.29; H, 5.28; N, 22.95, Found: C, 43.21; H, 5.37; N, 23.07. IR (KBr pellet): 2048 ν(N═N) (terminal), 1615 ν(C═N) cm^{-1}. λ_{max} (methanol) = 397 nm.

*Synthesis of $[MnL^2(N_3)_2]_n$ (**2**).* The procedure was the same as that for complex **1**, except that 5 mmol of a methanolic solution of the Schiff base ligand HL^2 (10 mL) was added instead of HL^1. The solution turned red immediately. On storing the resulting solution in a refrigerater, red colored, X-ray quality, prismatic shaped single crystals were obtained after two days.

Complex **2**. Yield: 0.950 g. (74%). $C_{22}H_{30}Mn_2N_{16}O_2$ (660.46) calcd: C, 40.01; H, 4.58; N, 33.94. Found: C, 40.11; H, 4.57; N, 33.87. IR (KBr pellet): 2065 ν(N═N) (bridging), 2050 ν(N═N) (terminal), 1627 ν(C═N) cm^{-1}. λ_{max} (methanol) = 401 nm.

Physical Measurements. Elemental analyses (C, H, and N) were performed using a Perkin-Elmer 240C elemental analyzer. IR spectra in KBr pellets (4500−500 cm^{-1}) were recorded using a Perkin-Elmer RXI FT-IR spectrophotometer. Electronic spectra in methanol (1000−200 nm) were recorded in a Hitachi U-3501 spectrophotometer. The DC magnetic susceptibility measurements were carried out in the temperature range 2−300 K with different applied magnetic fields in the range 0.01−5 T on polycrystalline samples of compounds **1** and **2** (with masses of 43.39 and 38.20 mg, respectively) with a Quantum Design MPMS-XL-5 SQUID susceptometer. AC suscetibility measurements were performed for sample **2** in the frequency range 0.1−10 kHz with an alternating field of 16 mT in the presence of DC fields in the range 0.01−2 T with a Quantum Design PPMS-9 system. The isothermal magnetizations were performed on the same samples in the temperature range 2−14 K with magnetic fields up to 5 or 8 T. The susceptibility data were corrected for the sample holders previously measured using the same conditions and for the diamagnetic contributions of the salts, as deduced by using Pascal's constant tables (χ_{dia} = −137.76 × 10^{-6} and −147.78 × 10^{-6} emu mol^{-1} for **1** and **2**, respectively).[24]

Crystal Data Collection and Refinement. A total of 4011 and 8236 independent reflection data were collected with Mo Kα radiation at 150 K using the Oxford Diffraction X-Calibur CCD System. The

dx.doi.org/10.1021/ic300274n | Inorg. Chem. 2012, 51, 5332−5341

crystals were positioned at 50 mm from the CCD. A total of 321 frames were measured with a counting time of 10 s. Data analyses were carried out with the CrysAlis program.[25] The structures were solved using direct methods with the Shelxs97 program.[26] The non-hydrogen atoms were refined with anisotropic thermal parameters. The hydrogen atoms bonded to carbon were included in geometric positions and given thermal parameters equivalent to 1.2 times those of the atom to which they were attached. Absorption corrections were carried out using the ABSPACK program.[27] Crystal data and structure refinement parameters of complexes **1** and **2** are given in Table 1.

Table 1. Crystal Data and Structure Refinement of Complexes 1 and 2

	1	2
formula	$C_{22}H_{32}Mn_2N_{10}O_4$	$C_{22}H_{30}Mn_2N_{16}O_2$
M	610.46	660.50
cryst syst	monoclinic	monoclinic
space group	$P2_1/c$	$P2_1/c$
a/Å	9.036(5)	6.7361(3)
b/Å	11.590(14)	19.6039(14)
c/Å	13.339(15)	21.5481(17)
β/deg	96.52(10)	95.929(5)
V/Å^3	1388(2)	2830.3(3)
Z	2	4
temp (K)	150	150
D_c/g cm^{-3}	1.461	1.550
μ/mm^{-1}	0.957	0.946
F (000)	632	1360.0
R(int)	0.072	0.099
total reflns	8588	19740
unique reflns	4011	8236
$I > 2\sigma(I)$	1691	3356
R1, wR2	0.0474, 0.0983	0.0536, 0.1068

RESULTS AND DISCUSSION

Synthesis of the Complexes. The two new Mn(III) complexes $[MnL^1(N_3)(OMe)]_2$ (**1**) and $[MnL^2(N_3)_2]_n$ (**2**) have been prepared with the tridentate Schiff base ligands HL^1 and HL^2, respectively, following a similar method: manganese-(II) acetate was allowed to react with the corresponding Schiff base and sodium azide in 1:1:2 molar ratios in methanol under ambient conditions to yield compounds **1** and **2** as red crystalline solids within a few hours, on keeping the solutions in a refrigerater. However, the compositions and structures of the compounds are very different. In **2**, one deprotonated tridentate Schiff base ligand and two azide ions coordinate to the Mn(III) centers, to provide a neutral complex. Of these two azides, one remains terminally coordinated while the other acts as a $\mu_{1,3}$-bridge to produce the one-dimensional chain structure. On the other hand, in **1**, a deprotonated methanol coordinates to the metal center instead of an azide ion and forms a double methoxido-bridged Mn(III) dimer. (Scheme 2).

IR and UV−vis Spectra of the Complexes. Spectroscopic data and their assignments are given in the Experimental Section. The IR spectra of the two complexes are very similar and show a strong and sharp peak corresponding to ν(C═N) at 1615 and 1627 cm^{-1} for complexes **1** and **2**, respectively, confirming the presence of the Schiff base. In the spectrum of complex **1**, a strong band at 2048 cm^{-1} is indicative of the presence of the N-coordinated terminal azide. While two overlapping but distinct peaks at 2050−2065 cm^{-1} for complex **2** corroborate the presence of two types of azido ligands (terminal and $\mu_{1,3}$ bridges). For complex **1**, a N−H stretching mode is observed at 3244 as a sharp band. The electronic spectra in methanolic solution of the two complexes display a single absorption band at 397 and 401 nm for complexes **1** and **2**, respectively. The positions of these bands are consistent with those reported in hexacoordinated Mn(III) complexes.[4b]

Description of Structures of the Complexes. *$[MnL^1(N_3)(OMe)]_2$ (**1**).* The structure of compound **1** is formed by a centrosymmetric methoxido-bridged Mn(III) dimer as shown in Figure 1. Bond distances and bond angles are given in Table 2.

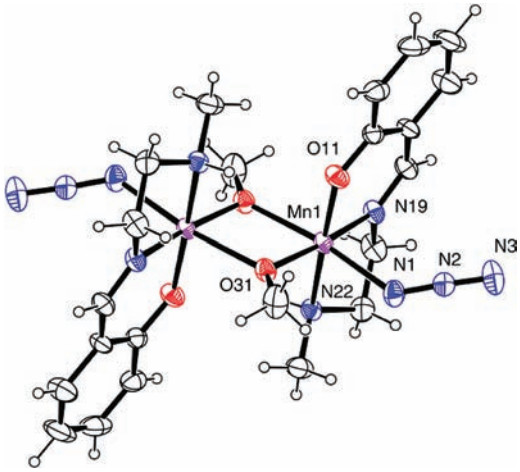

Figure 1. The structure of the centrosymmetric dimer **1** with ellipsoids at 30% probability.

Table 2. Bond Distances (Å) and Angles (deg) in the Metal Coordination Spheres of Compound 1

atoms	distance
Mn1−O11	1.887(3)
Mn1−O31	1.894(3)
Mn1−N19	1.992(4)
Mn1−N22	2.098(3)
Mn1−N1	2.174(4)
Mn1−O31^a	2.233(4)
atoms	**angle**
O11−Mn1−O31	92.07(13)
O11−Mn1−N19	91.32(14)
O31−Mn1−N19	171.09(10)
O11−Mn1−N22	172.51(11)
O31−Mn1−N22	94.52(14)
N19−Mn1−N22	81.66(14)
O11−Mn1−N1	95.32(13)
O31−Mn1−N1	96.61(15)
N19−Mn1−N1	91.28(15)
N22−Mn1−N1	87.46(13)
O11−Mn1−O31^a	90.45(12)
O31−Mn1−O31^a	78.42(14)
N19−Mn1−O31^a	93.32(14)
N22−Mn1−O31^a	86.40(12)
N1−Mn1−O31^a	172.54(9)

^{a}Symmetry element $1 - x, -y, 2 - z$.

dx.doi.org/10.1021/ic300274n | Inorg. Chem. 2012, 51, 5332−5341

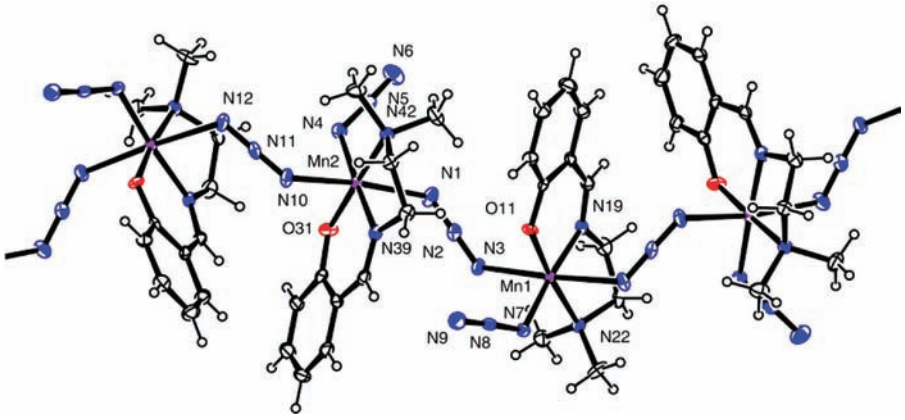

Figure 2. The structure of **2** with ellipsoids at 30% probability.

The metal atom occupies a distorted octahedral coordination sphere being meridionally coordinated to the L^1 ligand through O11, N19, and N22, together with a terminal azide N1 and two methoxido ligands, O31 and O31[a], acting as bridges between the two Mn(III) metal ions. The two bridging Mn−O bond distances are significantly different Mn1−O31 = 1.894(3) Å and Mn1−O31[a] = 2.233(4) Å. The short bond is trans to the azido ligand, whereas the longer one is trans to an imino nitrogen atom of the ligand. The manganese−azide bond is also longer than usual (Mn1−N1 = 2.174(4) Å). The azido ligand is quasi-linear, with a N−N−N angle of 176.7(4)°. Bond lengths to the tridentate ligand are in the normal range: Mn1−O11 = 1.887(3) Å, Mn1−N19 = 1.992(4) Å, and Mn1−N22 = 2.098(3) Å. The four donor atoms in the equatorial plane (O11, N19, N22, and O31) are nearly coplanar with an RMS deviation of 0.044(2) Å. The manganese atom is 0.041(1) Å from this plane in the direction of N19. Within the dimer, the Mn−Mn separation is 3.205(1) Å, and the distance between the two bridging oxygen atoms is 2.622(4) Å. The μ-O bridge in this complex forms a perfectly planar although asymmetric $Mn_2(\mu\text{-}O)_2$ ring since the dimer sits on a crystallographic inversion center. The Mn−O−Mn angle is 101.59(13)°. The phenyl rings are almost perpendicular to the planar $Mn_2(\mu\text{-}O)_2$ core with a dihedral angle of 88.99(8)°. Two phenyl rings are coplanar to each other. The donor H22 atom of the imine nitrogen of a dinuclear compound participate in intermolecular hydrogen bonding with an acceptor N3[c] atom of a terminal azido of a neighboring dimer (H···A = 2.49 Å, D···A = 3.276(7) Å, D−H···A angle =145°; c = x, 1/2 − y, 1/2 + z) to form the 2D supramolecular architecture shown in Figure S1.

$[MnL^2(N_3)_2]_n$ (**2**). The structure of compound **2** is formed by a linear Mn(III) chain, as shown in Figure 2. Bond distances and angles are given in Table 3.

There are two metal atoms in the asymmetric unit, but they have identical coordination spheres. Both present an octahedral geometry with a meridionally bonded tridentate ligand L^{2-}, together with one terminal and two $\mu_{1,3}$-N_3 bridges. The three donor atoms of the Schiff base, along with the coordinated nitrogen atom of the terminal azido ligand, constitute the equatorial planes in both Mn atoms. The bridging azides (N1 and N10 atoms in Mn2 and N3 and N12 atoms in Mn1) are coordinated in the two trans axial positions. Bond lengths to the ligand L^2 are equivalent for the two Mn atoms (Mn1−O11 = 1.878(2) Å, Mn1−N19 = 1.991(3) Å, and Mn1−N22 = 2.113(3) Å, very close to those of Mn2: Mn2−O31 = 1.883(2) Å, Mn2−N39 = 1.980(3) Å, and Mn2−N42 = 2.110(3) Å). It is also noteworthy that the bonds to the terminal azido bridges, Mn1−N7 = 1.941(3) Å and Mn2−N4 = 1.945(3) Å, are significantly shorter than the bonds to the bridging azido ones, Mn1−N3 = 2.280(3) Å, Mn1−N12[b] = 2.297(3) Å, Mn2−N1 = 2.275(3) Å, and Mn2−N10 = 2.277(3) Å, as a consequence of the Jahn−Teller distortion in the Mn(III) ion. The RMS deviations of the four equatorial atoms from the mean plane passing through them are 0.009 and 0.015 Å for Mn1 and Mn2, respectively. The metal atoms are 0.041(1) and 0.017(1) Å from this plane toward N3 and N1 atoms for Mn1 and Mn2, respectively. The dihedral angle between these two equatorial planes is 58.5(1)°. The Mn−Mn separation within the chain is 5.958(1) Å. It is interesting to note that each single $\mu_{1,3}$-N_3 bridge between Mn1 and Mn2 induces helicity in the chain along the c direction. However, as the compound crystallizes in an achiral space group, there is an equal number of right and left handed helical chains (Figure S2). This kind of helical chain propagating through single azido-bridged metal ions is reported

Table 3. Bond Distances (Å) and Angles (deg) in the Metal Coordination Spheres of Compound 2

atoms	distance	atoms	distance
Mn1−O11	1.878(2)	Mn2−O31	1.883(2)
Mn1−N7	1.941(3)	Mn2−N4	1.945(3)
Mn1−N19	1.991(3)	Mn2−N39	1.980(3)
Mn1−N22	2.113(3)	Mn2−N42	2.110(3)
Mn1−N3	2.280(3)	Mn2−N1	2.275(3)
Mn1−N12[b]	2.297(3)	Mn2−N10	2.277(3)
atoms	**angle**	**atoms**	**angle**
O11−Mn1−N7	93.92(10)	O31−Mn2−N4	91.65(11)
O11−Mn1−N19	91.66(10)	O31−Mn2−N39	91.86(11)
N7−Mn1−N19	174.06(12)	N4−Mn2−N39	176.49(12)
O11−Mn1−N22	173.79(10)	O31−Mn2−N42	175.54(10)
N7−Mn1−N22	91.55(11)	N4−Mn2−N42	92.40(11)
N19−Mn1−N22	82.77(11)	N39−Mn2−N42	84.08(11)
O11−Mn1−N3	88.70(10)	O31−Mn2−N1	90.11(11)
N7−Mn1−N3	90.71(11)	N4−Mn2−N1	94.82(11)
N19−Mn1−N3	91.44(10)	N39−Mn2−N1	85.37(11)
N22−Mn1−N3	94.16(10)	N42−Mn2−N1	91.40(11)
O11−Mn1−N12[b]	89.62(10)	O31−Mn2−N10	90.23(11)
N7−Mn1−N12[b]	92.57(11)	N4−Mn2−N10	94.45(11)
N19−Mn1−N12[b]	85.43(11)	N39−Mn2−N10	85.33(11)
N22−Mn1−N12[b]	87.22(10)	N42−Mn2−N10	87.61(11)
N3−Mn1−N12[b]	176.41(11)	N1−Mn2−N10	170.71(11)

[b]Symmetry element x, 0.5 − y, −0.5 + z.

dx.doi.org/10.1021/ic300274n | *Inorg. Chem.* 2012, 51, 5332−5341

in the literature.[20a,f,g,28] The 1D chains are interconnected by weak C13−H13···N2 and C421−H42F···N6 hydrogen bonds to produce a 2D supramolecular structure (Figure 3 and Table

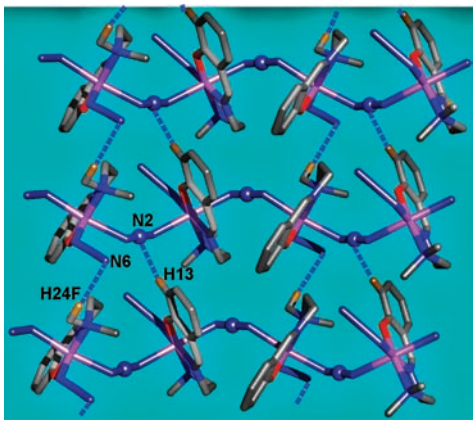

Figure 3. C−H···N hydrogen bonded 2D network of compound **2**.

Table 4. Hydrogen Bond Interactions in Complex 2

D−H···A	D−H (Å)	H···A (Å)	D···A (Å)	∠D−H···A (deg)	symmetry
C13−H13···N2	0.93	2.57	3.481(4)	165	1 + *x*, *y*, *z*
C421−H42F···N6	0.96	2.60	3.522(5)	160	1 + *x*, *y*, *z*

4) with distances of 3.481(4) and 3.522(5) Å, respectively. These interactions seem to have an important effect on the magnetic properties of complex **2**, which are discussed below.

Magnetic Properties. *Complex [MnL^1(N$_3$)(OMe)]$_2$ (**1**).* The thermal variation of the molar magnetic susceptibility per Mn(III) dimer times the temperature ($\chi_m T$) for compound **1** shows at room temperature a value of *ca.* 5.9 emu K mol^{-1}, very close to the expected one for two S = 2 Mn(III) isolated ions (6.0 emu K mol^{-1} for g = 2). When the temperature is decreased, $\chi_m T$ remains constant down to ca. 150 K, and below this temperature, $\chi_m T$ increases to reach a value of ca. 9.6 emu K mol^{-1} at *ca.* 2 K (Figure 4). This behavior is indicative of predominant ferromagnetic exchange interactions inside the Mn(III) dimer present in this compound. Accordingly, we have used a simple S = 2 dimer model, which reproduces very satisfactorily the magnetic data in the whole temperature range with g = 1.982 and J = 0.95 cm^{-1} (the Hamiltonian is written as

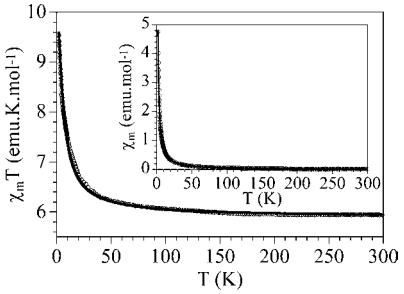

Figure 4. Thermal variation of the $\chi_m T$ product for compound **1**. Inset shows the thermal variation of χ_m. Solid line represents the best fit to the model (see text).

$H = -JS_1S_2$; solid line in Figure 4). Note that the presence of a weak zero field splitting cannot be excluded. In fact, a low D value has been observed in similar Mn(III) dimers with this kind of asymmetric oxido bridge.[2a,c,d] Nevertheless, the values of both parameters are similar and closely correlated, precluding a reliable simultaneous fit of both parameters.

The weak ferromagnetic coupling observed in compound **1** can be easily rationalized from the structural parameters of the double asymmetric oxido bridge (see above). This double bridge shows a long (2.233(4) Å) and a short (1.894(3) Å) Mn−O bond distance due to the presence of a Jahn−Teller distortion in the d^4 Mn(III) center along one of the Mn−O bridging bonds, leading to a poor overlap of the magnetic orbitals that results in a very weak coupling, as observed experimentally. This result agrees with the weak ferromagnetic couplings found in similar Mn(III) dimers with double asymmetric oxido bridges.[2a,c,d,29,30]

*Complex [MnL^2(N$_3$)$_2$]$_n$ (**2**).* The thermal variation of the molar magnetic susceptibility per Mn(III) ion times the temperature ($\chi_m T$) for compound **2** shows at room temperature a value of ca. 2.5 emu K mol^{-1} (Figure 5), slightly below

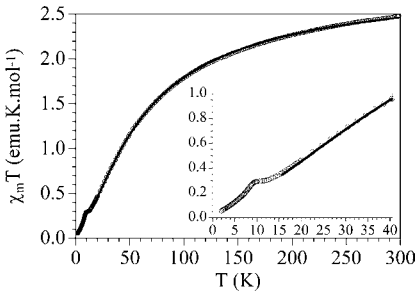

Figure 5. Thermal variation of the product of the molar magnetic susceptibility per Mn(III) ion times the temperature, $\chi_m T$, for compound **2** at 0.1 T. Inset shows the low temperature region. Solid line represents the best fit to the model (see text).

the expected one for one isolated Mn(III) S = 2 ion with g = 2.0. When the temperature is lowered, the $\chi_m T$ product shows a progressive decrease and reaches a value of ca. 0.05 emu K mol^{-1} at 2 K. A close inspection of this plot shows a small hint at *ca.* 10 K, indicative of a transition to a long-range ordering (inset in Figure 5). The decrease observed in the $\chi_m T$ product indicates the presence of predominant antiferromagnetic exchange interactions in compound **2**. Given the chain structure shown by this compound and the structural similitude of the $\mu_{1,3}$-N$_3$ bridges connecting the Mn(III) ions, we have used the simple S = 2 regular antiferromagnetic chain model derived by Ficher[31] to fit the magnetic properties:

$$\chi_{chain} = \frac{Ng^2\beta^2S(S+1)}{3kT}\frac{1+u}{1-u} \text{ with } u = \coth\left[\frac{JS(S+1)}{kT}\right] - \left[\frac{kT}{JS(S+1)}\right]$$

where J is the intrachain coupling constant and S = 2 in this case.

This simple model reproduces very satisfactorily the magnetic properties of compound **2** above ca. 15 K (solid line in Figure 5) with g = 1.967 and J = −8.5 cm^{-1} (the Hamiltonian is written as $H = -JS_iS_{i+1}$). Note that although the two intrachain bridges are not identical, they are very similar,

dx.doi.org/10.1021/ic300274n | Inorg. Chem. 2012, 51, 5332−5341

and in order to reduce the number of adjustable parameters, we have assumed that they are equivalent. The very satisfactory fit obtained with the model confirms that this assumption is acceptable.

The small kink observed in the $\chi_m T$ product at ca. 10 K can be more clearly seen in the χ_m plot (Figure 6) as a sharp peak at

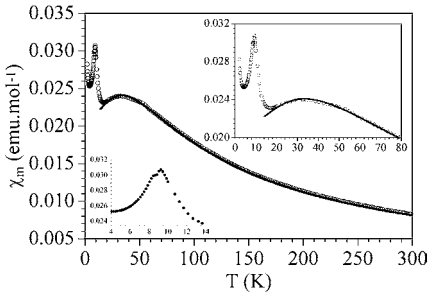

Figure 6. Thermal variation of the molar magnetic susceptibility per Mn(III) ion for compound **2** at 0.1 T. The upper inset shows the low temperature region. Lower inset shows a detail of the peak at *ca.* 9.3 K and the shoulder at *ca.* 8.5 K. Solid line represents the best fit to the model (see text).

9.3 K, suggesting the presence of antiferromagnetic long-range ordering taking place at 9.3 K. At lower temperatures, the χ_m plot shows a Curie tail arising from the presence of monomeric paramagnetic impurities resulting from crystal defects and vacancies in the chain.

In order to investigate the exact nature of the peak observed in the susceptibility plot at ca. 9.3 K, we have performed AC susceptibility measurements at different frequencies (Figure 7). These measurements show a frequency-independent maximum only observed in the in-phase signal (χ_m') at ca. 9.3 K, also observed in the DC measurements, corresponding to the antiferromagnetic long-range ordering. Besides this peak, the in phase (χ_m') and out of phase (χ_m'') signals show a narrow peak at lower temperatures (*ca.* 8.5 K) whose position is frequency-independent but with an intensity that increases as the frequency is decreased. This narrow peak corresponds to either a ferromagnetic or a canted antiferromagnetic (weak ferromagnetic) long-range ordering.[32−34] Since the coupling observed in **2** is antiferromagnetic (see above), this peak has to be attributed to the presence of a long-range canted antiferromagnetic order, as already observed in several other Mn(III) chain compounds.[4b,22,35−41] This canted antiferromagnetic long-range order appears when the single ion anisotropy axes are not parallel, as is commonly observed in Mn(III) chains when the ions present a tetragonal elongated environment with four short basal bonds and two longer axial ones.[4b,35−37,40,41] In fact, in compound **2**, there are two crystallographically independent Mn(III) centers that present axial directions not colinear with the helical chain axis (see above). Interestingly, a close look at the DC measurement (lower inset in Figure 6) shows that the peak observed at *ca.* 9.3 K also presents a shoulder at ca. 8.5 K corresponding to the canted antiferromagnetic ordering. We can, therefore, assume that the ordering process takes place in two distinct steps: first, all the spins along the chain align antiparallelly and order antiferromagnetically at 9.3 K, and in a second step, the single ion anisotropy slightly rotates the spins to give a canted antiferromagnetic order, responsible for the frequency-independent peak at 8.5 K.

In order to study the unusual frequency dependence of the intensity of the χ_m'' peak at 8.5 K, we have performed AC measurements at many different frequencies (inset in Figure 7). These measurements show that the intensity decreases as the frequency increases in a double linear way with the logarithm of the frequency (left inset in Figure 7). Interestingly, similar behavior has very recently been observed in a related Mn(III) canted antiferromagnetic chain[4b] and in the magnetic $Nd_{60}Fe_{30}Al_{10}$ alloys, where this behavior is attributed to the presence of a distribution of relaxation times, τ, and to the fact that τ is larger than $1/\nu$.[42] Note that this frequency dependence of the intensity of the χ_m' and χ_m'' peaks cannot be attributed to the movement of the domain walls along the chain since its position is frequency independent.

Further proof of the canted antiferromagnetic long-range order is provided by the isothermal magnetization measurements at different temperatures above and below the transition temperature (Figures 8 and 9). These measurements show a

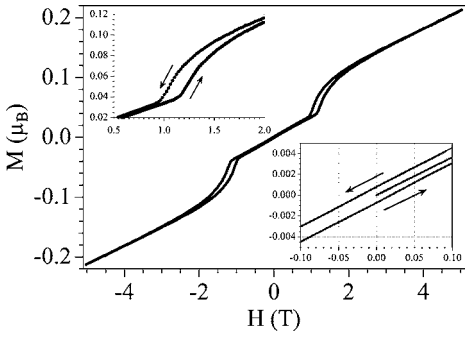

Figure 8. Isothermal magnetization of **2** at 2 K. Insets show the low field region and the metamagnetic transition near 1.0 T.

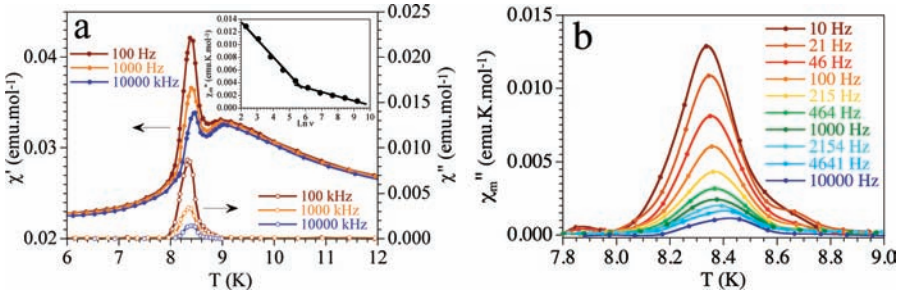

Figure 7. (a) Thermal variation of the in-phase (χ_m', filled circles, left scale) and out-of-phase (χ_m'', empty circles, right scale) susceptibilities for compound **2** at different frequencies. Inset shows the dependence of the maximum of the intensity of the χ_m'' signal with the Ln ν. (b) χ_m'' signal at different frequencies in the 10−10 000 Hz range.

dx.doi.org/10.1021/ic300274n | *Inorg. Chem.* 2012, 51, 5332−5341

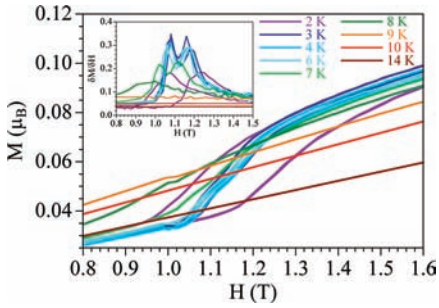

Figure 9. Isothermal magnetization of **2** at different temperatures. Inset shows the magnetic field dependence of the derivative of the magnetization with the magnetic field near the critical field.

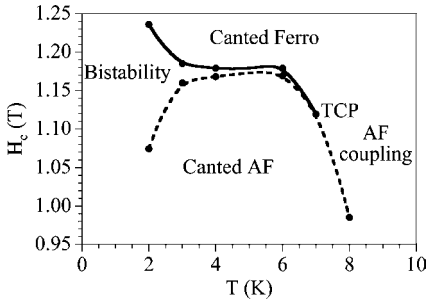

Figure 10. Phase diagram of **2** showing the antiferromagnetically coupled phase at high temperatures and low fields, the canted antiferromagnetic phase at low temperatures and low fields, and the canted ferromagnetic phase at high fields and low temperatures.

linear increase of the magnetization with increasing the magnetic field and a very low value at high fields (*ca.* 0.2 μ_B at 5 T, well below the expected value of *ca.* 4.0 μ_B per Mn(III) ion), in agreement with the antiferromagnetic coupling observed in this compound. Furthermore, the magnetization measurements show a hysteresis cycle with a coercive field of *ca.* 20 mT at 2 K (right inset in Figure 8) that confirms the weak ferromagnetic long-range ordering in compound **2**. This coercive field decreases as the temperature increases and vanishes above *ca.* 7 K. At 2 K, the magnetization shows an abrupt increase at ca. 1.2 T with an increase from *ca.* 0.04 μ_B at 1.1 T to ca. 0.10 μ_B at 1.5 T (left inset in Figure 8). For fields above 1.5 T, the magnetization shows again a linear behavior with a similar slope to the one observed at low fields. This jump in the magnetization at ca. 1.25 T suggests the presence of a metamagnetic transition with a critical field of *ca.* 1.25 T. However, at 2 K the critical field is different in the increasing and decreasing field scans (left inset in Figure 8), with values of ca. 1.24 and 1.08 T, respectively, as observed in the derivatives of the magnetization with the magnetic field (inset in Figure 9).

A detailed study of the thermal variation of the critical field of the metamagnetic transition (Figure 9) shows that (i) the hysteresis in the critical field decreases very fast as the temperature is increased and vanishes above *ca.* 6 K, (ii) the critical field also decreases, although less abruptly, when the temperature is increased and disappears above *ca.* 8 K (Figure 9), and (iii) the metamagnetic transition has two very close critical fields in both scans in the temperature range 3−7 K (inset in Figure 9). The difference between both critical fields is close to 0.1 T at any temperature, suggesting that they might be related to the presence of two different interchain antiferromagnetic interactions corresponding to the two directions perpendicular to the chain axis (see above).

The study of the variation of the critical field with the temperature leads to the phase diagram shown in Figure 10. This diagram shows that compound **2** is a canted antiferromagnet at low fields and low temperatures, as a result of a canted antiferromagnetic intrachain coupling (through the $\mu_{1,3}$-N_3 bridges). These chains present a weak interchain antiferromagnetic coupling (through weak H bonds along the *x* and *y* directions, see Table 4) that can be overpassed with a moderate magnetic field of *ca.* 1.2 T at 2 K, corresponding to the observed metamagnetic transition. The tricritical point (TCP) in this diagram, where the three phases coexist (the canted antiferro- and ferromagnetic and the nonordered antiferrommagnetic ones), belongs to the $H_c = f(T)$ line. In our case, this point is located at *ca.* 7 K, which is the temperature at which the metamagnetic transition loses the hysteretic behavior. At temperatures below the critical point, the metamagnetic transition presents hysteresis and is a first order transition, whereas at temperatures above the TCP, the metamagnetic transition is second order and does not present hysteresis.[43,44] The area where the hysteresis takes place corresponds to the region of bistability where the two states may exist depending on the conditions.

In order to better study the field dependence on the magnetic ground state in **2**, we have performed a more complete study of the DC and AC magnetic susceptibilities as a function of the applied DC magnetic field. These measurements show that the DC magnetic susceptibility shows a peak at *ca.* 9.3 K for fields below *ca.* 1.0 T (Figure 11), but for fields

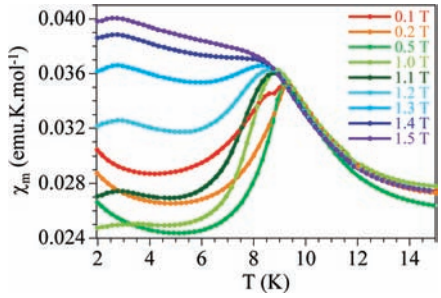

Figure 11. Thermal variation of the molar susceptibility of compound **2** with different applied magnetic fields.

above *ca.* 1.0 T the peak shifts to lower temperatures and disappears above *ca.* 1.4 T. This behavior indicates that the interchain antiferromagnetic coupling is canceled by magnetic fields above *ca.* 1.4 T, as observed in the isothermal magnetization measurements. The lack of saturation of the susceptibility at low temperatures confirms the presence of a spin canting in the ferromagnetic phase.

The AC measurements also show a very different behavior when a DC magnetic field is applied simultaneously to the AC oscillating field (Figure 12). Thus, the peak observed at *ca.* 8.5 K in the χ_m'' signal disappears for any applied magnetic field above 0.01 T (inset in Figure 12), indicating that the small canting angle observed in the antiferromagnetic ordered phase is suppressed by the application of a weak magnetic field. As expected, the application of higher DC magnetic fields, near the metamagnetic transition, leads to the appearance of a novel χ_m' signal, now at lower temperatures, ca. 7.0 K, that corresponds to the interchain long-range ferromagnetic ordering induced by the DC magnetic fields above the critical field of *ca.* 1.2−1.3 T (Figure 13). This new in-phase signal is also accompanied by

dx.doi.org/10.1021/ic300274n | *Inorg. Chem.* 2012, 51, 5332−5341

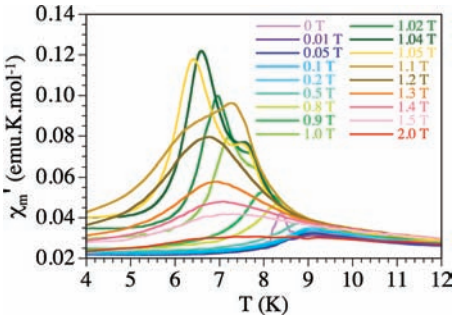

Figure 12. Thermal variation of χ_m' of compound **2** at 10 kHz with different applied DC fields.

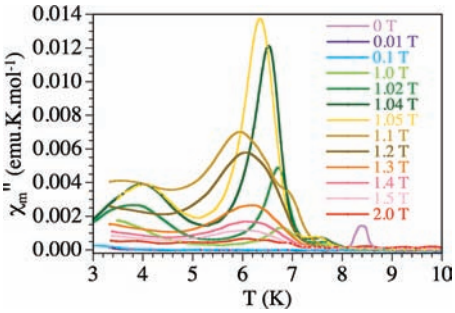

Figure 13. Thermal variation of χ_m'' of compound **2** at 10 kHz with different applied DC fields.

the corresponding out-of-phase signal, which confirms the long-range ferromagnetic ordering observed at *ca.* 7 K.

Confirmation of the presence of two close critical fields for the metamagnetic transition comes from the measurement of the AC magnetization as a function of the applied DC field at a fixed temperature (Figure 14). These measurements show that

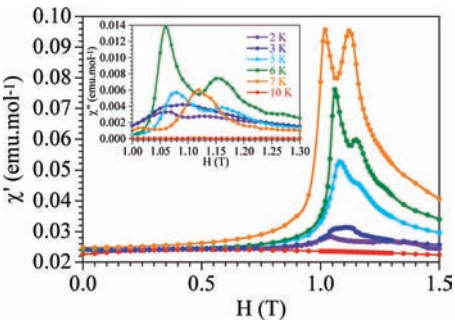

Figure 14. Isothermal (in phase, χ_m') AC magnetization of compound **2** at 10 kHz and different temperatures. Inset shows the out-of-phase (χ_m'') AC magnetization at the same temperatures.

at different temperatures in the 2−7 K range, the χ_m' signal presents two peaks or a peak and a shoulder at ca. 1.1 and ca. 1.2 T, in agreement with the DC magnetization measurements (see above). The χ_m'' signal shows a similar behavior although now the two peaks are more clearly observed at ca. 1.05 and 1.15 T, respectively (inset in Figure 14).

CONCLUSIONS

We have prepared two novel Mn(III) complexes with azido and NNO donor Schiff-base ligands. In compound **1**, the presence of coordinated methoxide groups has led to the formation of a Mn(III) dimer with a double methoxido bridge that yields a weak ferromagnetic coupling (J = 0.95 cm^{-1}). Compound **2** is a Mn(III) chain compound with $\mu_{1,3}$-azido bridges that presents a moderate (J = −8.5 cm^{-1}) antiferromagnetic coupling. At *ca.* 9.3 K, **2** shows an antiferromagnetic long-range order (as shown by the presence of a peak in χ_m and in χ_m' but not in χ_m'' at *ca.* 9.3 K). Albeit, the local anisotropy of the Mn(III) ions (that present an elongated tetragonal environment) prevents a complete antiparallel alignment of the spins. This canting angle of the local spins leads to a weak ferromagnetic long-range order that appears at *ca.* 8.5 K (as shown by the presence of a frequency-independent peak in χ_m'' at *ca.* 8.5 K). Below this temperature, the residual moments on the chains are antiferromagnetically coupled with those of the neighboring chains (in both directions perpendicular to the chain). This interchain coupling is overcome with the application of a magnetic field above *ca.* 1.1−1.2 T, leading to a long-range ferromagnetic order of the resulting magnetic moments on the chains. Therefore, **2** presents a metamagnetic transition at low temperatures with a critical field of *ca.* 1.1−1.2 T that changes the sign of the interchain interaction from antiferromagnetic to ferromagnetic. The critical field presents a hysteresis below *ca.* 6 K (corresponding to the tricritical point) that leads to the phase diagram depicted in Figure 10. Similar behavior has been observed in a cyanide bridged Cr−Ni metamagnet.[43] Note also that similar, although not identical, behavior has already been observed in other Co(II) and Mn(III) chain systems.[36,38,45,46]

ASSOCIATED CONTENT

Supporting Information

Hydrogen-bonded 2D supramolecular structure of complex **1**, helical structure of complex **2**, and a crystallogrphic information file. This material is available free of charge via the Internet at http://pubs.acs.org.

AUTHOR INFORMATION

Corresponding Author

*E-mail: ghosh_59@yahoo.com.

Notes

The authors declare no competing financial interest.

ACKNOWLEDGMENTS

We thank CSIR, India for awarding a senior research fellowship [Sanction No.09/028 (0732)/2008-EMR-I] to S.B. We also thank EPSRC and the University of Reading for funds for the X-Calibur system, the Spanish Ministerio de Economía y Competitividad (Projects Consolider-Ingenio in Molecular Nanoscience CSD2007-00010 and CTQ-2011-26507), and the Generalitat Valenciana (Project Prometeo 2009/95).

REFERENCES

(1) (a) Kahn, O. *Molecular Magnetism*; VCH: New York, 1993. (b) Gatteschi, D.; Sessoli, R. *Angew. Chem., Int. Ed.* **2003**, *42*, 268−297. (c) Gatteschi, D.; Sessoli, R.; Villain, J. *Molecular Nanomagnets*; Oxford University Press: Oxford, U.K., 2006. (d) Berchin, E. K. *Chem. Commun.* **2005**, 5141−5153. (e) Lescouëzec, R.; Toma, L. M.; Vaissermann, J.; Verdaguer, M.; Delgado, F. S.; Ruiz-Pérez, C.; Lloret, F.; Julve, M. *Coord. Chem. Rev.* **2005**, *249*, 2691−2729. (f) Hiraga, H.; Miyasaka, H.; Clerac, R.; Fourmigue, M.; Yamashita, M. *Inorg. Chem.* **2009**, *48*, 2887−2898. (g) Wu, D.; Guo, D.; Song, Y.; Huang, W.; Chunying, D.; Meng, Q.; Sato, O. *Inorg. Chem.* **2009**, *48*, 854−860.

(2) (a) Miyasaka, H.; Clerac, R.; Wernsdorfer, W.; Lecren, L.; Bonhomme, C.; Sugiura, K.; Yamashita, M. *Angew. Chem., Int. Ed.* **2004**, *43*, 2801−2805. (b) Schelter, E. J.; Prosvirin, A. V.; Dunbar, K.

R. *J. Am. Chem. Soc.* **2004**, *126*, 15004−15005. (c) Miyasaka, H.; Clerac, R.; Ishii, T.; Chang, H.; Kitagawa, S.; Yamashita, M. *J. Chem. Soc., Dalton Trans.* **2002**, 1528−1534. (d) Bhargavi, G.; Rajasekharan, M. V.; Costes, J.; Tuchagues, J. *Polyhedron* **2009**, *28*, 1253−1260. (e) Mondal, K. C.; Drew, M. G. B.; Mukherjee, P. S. *Inorg. Chem.* **2007**, *46*, 5625−5629.

(3) Miyasaka, H.; Matsumoto, N.; Okawa, H.; Re, N.; Gallo, E.; Floriani, C. *Angew. Chem., Int. Ed.* **1995**, *34*, 1446−1448.

(4) (a) Cringh, Y.; Gordon-Wylie, S. W.; Norman, R. E.; Clark, G. R.; Weintraub, S. T.; Horwitz, C. P. *Inorg. Chem.* **1997**, *36*, 4968−4982. (b) Kar, P.; Guha, P. M.; Drew, M.G. B.; Ishida, T.; Ghosh, A. *Eur. J. Inorg. Chem.* **2011**, 2075−2085.

(5) (a) Coulon, C.; Miyasaka, H.; Clerac, R. *Struct. Bonding (Berlin)* **2006**, *122*, 163−206. (b) Kar, P.; Biswas, R.; Drew, M. G. B.; Ida, Y.; Ishida, T.; Ghosh, A. *Dalton Trans.* **2011**, *40*, 3295−3304.

(6) (a) Adhikary, C.; Koner, S. *Coord. Chem. Rev.* **2010**, *254*, 2933−2958. (b) Wang, S.-B.; Yang, G.-M.; Li, R.-F.; Li, L.-C.; Liao, D.-Z. *Inorg. Chem. Commun.* **2004**, *7*, 1082−1085. (c) Gao, E.-Q.; Bai, S.-Q.; Yue, Y.-F.; Wang, Z.-M.; Yan, C.-H. *Inorg. Chem.* **2003**, *42*, 3642−3649. (d) Boudalis, A. K.; Sanakis, Y.; Clemente-Juan, J. M.; Donnadieu, B.; Nastopoulos, V.; Mari, A.; Coppel, Y.; Tuchagues, J. P.; Perlepes, S. P. *Chem.—Eur. J.* **2008**, *14*, 2514−2526. (e) Naiya, S.; Biswas, C.; Drew, M. G. B.; Gomez-García, C. J.; Clemente-Juan, J. M.; Ghosh, A. *Inorg. Chem.* **2010**, *49*, 6616−6627. (f) (a) Mukherjee, S.; Mukherjee, P. S. *Inorg. Chem.* **2010**, *49*, 10658−10667.

(7) (a) Stamatatos, T. C.; Papaefstathiou, G. S.; MacGillivray, L. R.; Escuer, A.; Vicente, R.; Ruiz, E.; Perlepes, S. P. *Inorg. Chem.* **2007**, *46*, 8843−8850. (b) Abu-Youssef, M. A. M.; Escuer, A.; Mautnerc, F. A.; Ohrstrom, L. *Dalton Trans.* **2008**, 3553−3558. (c) Naiya, S.; Biswas, S.; Drew, M. G. B.; Gómez-García, C. J.; Ghosh, A. *Inorg. Chim. Acta* **2011**, *377*, 26−33. (d) Biswas, C.; Drew, M. G. B.; Ruiz, E.; Estrader, M.; Diaz, C.; Ghosh, A. *Dalton Trans.* **2010**, *39*, 7474−7484. (e) Biswas, A.; Drew, M. G. B.; Gomez-García, C. J.; Ghosh, A. *Inorg. Chem.* **2010**, *49*, 8155−8163. (f) Mukherjee, S.; Gole, B.; Chakrabarty, R.; Mukherjee, P. S. *Inorg. Chem.* **2009**, *48*, 11325−11334. (g) Sengupta, O.; Mukherjee, P. S. *Inorg. Chem.* **2010**, *49*, 8583−8590.

(8) (a) Nanda, P. K.; Aromí, G.; Ray, D. *Chem. Commun.* **2006**, 318−323. (b) Lazari, G.; Stamatatos, T. C.; Raptopoulou, C. P.; Psycharis, V.; Pissas, M.; Perlepes, S. P.; Boudalis, A. K. *Dalton Trans.* **2009**, 3215−3221. (c) Chattopadhyay, S.; Ray, M. S.; Drew, M. G. B.; Figuerola, A.; Diaz, C.; Ghosh, A. *Polyhedron* **2006**, *25*, 2241−2253.

(9) (a) Goher, M. A. S.; Mautner, F. A. *Polyhedron* **1995**, *14*, 1439−1446. (b) Gu, Z.-G.; Xu, Y.-F.; Yin, X.-J.; Zhou, X.-H.; Zuo, J.-L.; You, X.-Z. *Dalton Trans.* **2008**, 5593−5602. (c) Zhang, X.-M.; Zhao, Y.-F.; Wu, H.-S.; Battenb, S. R.; Ng, S. W. *Dalton Trans.* **2006**, 3170−3178. (d) Guo, G. C.; Mak, T. C. W. *Angew. Chem., Int. Ed.* **1998**, *37*, 3268−3270.

(10) (a) Tandon, S. S.; Thompson, L. K.; Manuel, M. E.; Bridson, J. N. *Inorg. Chem.* **1994**, *33*, 5555−5570. (b) Ribas, J.; Escuer, A.; Monfort, M.; Vicente, R.; Cortes, R.; Lezama, L.; Rojo, T. *Coord. Chem. Rev.* **1999**, *193*−*195*, 1027−1068. (c) Naiya, S.; Drew, M. G. B.; Diaz, C.; Ribas, J.; Ghosh, A. *Eur. J. Inorg. Chem.* **2011**, 4993−4999.

(11) (a) Zbiri, M.; Saha, S.; Adhikary, C.; Chaudhuri, S.; Daul, C.; Koner, S. *Inorg. Chim. Acta* **2006**, *359*, 1193−1199. (b) Mukherjee, P. S.; Dalai, S.; Mostafa, G.; Lu, T.-H.; Rentschlerc, E.; Chaudhuri, N. R. *New J. Chem.* **2001**, *25*, 1203−1207. (c) Manikandan, P.; Muthukumaran, R.; Justin Thomas, K. R.; Varghese, B.; Chandramouli, G. V. R.; Manoharan, P. T. *Inorg. Chem.* **2001**, *40*, 2378−2389. (d) Ray, M. S.; Ghosh, A.; Bhattacharya, R.; Mukhopadhyay, G.; Drew, M. G. B.; Ribas, J. *Dalton Trans.* **2004**, 252−259.

(12) Das, A.; Rosair, G. M.; El Fallah, M. S.; Ribas, J.; Mitra, S. *Inorg. Chem.* **2006**, *45*, 3301−3306.

(13) Hong, C. S.; Koo, J.-E.; Son, S.-K.; Lee, Y. S.; Kim, Y.-S.; Do, Y. *Chem.—Eur. J.* **2001**, *7*, 4243−4252.

(14) You, Y. S.; Yoon, J. H.; Kim, H. C.; Hong, C. S. *Chem. Commun.* **2005**, 4116−4118.

(15) (a) Zhou, A. J.; Qin, L. J.; Beedle, C. C.; Ding, S.; Nakano, M.; Leng, J. D.; Tong, M. L.; Hendrickson, D. N. *Inorg. Chem.* **2007**, *46*, 8111−8113. (b) Ge, C. H.; Cui, A. L.; Ni, Z. H.; Jiang, Y. B.; Zhang, L. F.; Ribas, J.; Kou, H. Z. *Inorg. Chem.* **2006**, *45*, 4883−4885. (c) Wang, M.; Ma, C.; Chen, C. *Dalton Trans.* **2008**, 4612−4620. (d) Yang, P. P.; Wang, X. L.; Li, L. C.; Liao, D. Z. *Dalton Trans.* **2011**, *40*, 4155−4161.

(16) (a) Nastase, S.; Tuna, F.; Maxim, C.; Muryn, C. A.; Avarvari, N.; Winpenny, R. E. P.; Andruh, M. *Cryst. Growth Des.* **2007**, *7*, 1825−1831. (b) Hewitt, I. J.; Tang, J. K.; Madhu, N. T.; Clerac, R.; Buth, G.; Anson, C. E.; Powell, A. K. *Chem. Commun.* **2006**, 2650−2652. (c) Mialane, P.; Duboc, C.; Marrot, J.; Riviere, E.; Dolbecq, A.; Secheresse, F. *Chem.—Eur. J.* **2006**, *12*, 1950−1959.

(17) Hoshino, N.; Ito, T.; Nihei, M.; Oshio, H. *Inorg. Chem. Commun.* **2003**, *6*, 377−380.

(18) Wemple, M. W.; Adams, D. M.; Hagen, K. S.; Folting, K.; Hendrickson, D. N.; Christou, G. *Chem. Commun.* **1995**, 1591−1594.

(19) (a) Liu, C. M.; Zhang, D. Q.; Zhu, D. B. *Chem. Commun.* **2008**, 368−370. (b) Viciano-Chumillas, M.; Tanase, S.; Mutikainen, I.; Turpeinen, U.; de Jongh, L. J.; Reedijk, J. *Inorg. Chem.* **2008**, *47*, 5919−5929. (c) Xu, H. B.; Wang, B. W.; Pan, F.; Wang, Z. M.; Gao, S. *Angew. Chem., Int. Ed.* **2007**, *46*, 7388−7392. (d) Song, X.; Yang, P. P.; Mei, X.; Li, L.; Liao, D. Z. *Eur. J. Inorg. Chem.* **2010**, 1689−1695.

(20) (a) Reddy, K. R.; Rajasekharan, M. V.; Tuchagues, J. P. *Inorg. Chem.* **1998**, *37*, 5978−5982. (b) Darensbourg, D. J.; Frantz, E. B. *Inorg. Chem.* **2007**, *46*, 5967−5978. (c) Li, W.; Li, Z.; Li, L.; Liao, D.; Jiang, Z. *J. Solid State Chem.* **2007**, *180*, 2973−2977. (d) Stults, B. R.; Marianelli, R. S.; Day, V. W. *Inorg. Chem.* **1975**, *14*, 722−723. (e) Feng, Y. L. *Chin. J. Struct. Chem.* **2002**, *21*, 352−354. (f) Ko, H. H.; Lim, J. H.; Kim, H. C.; Hong, C. S. *Inorg. Chem.* **2006**, *45*, 8847−8849. (g) Yuan, M.; Zhao, F.; Zhang, W.; Wang, Z. M.; Gao, S. *Inorg. Chem.* **2007**, *46*, 11235−11242. (h) Panja, A.; Shaikh, N.; Vojtisek, P.; Gao, S.; Banerjee, P. *New J. Chem.* **2002**, *26*, 1025−1028. (i) Zhang, Y.; Wang, X. T.; Zhang, X. M.; Liu, T. F.; Xu, W. G.; Gao, S. *Inorg. Chem.* **2010**, *49*, 5868−5875.

(21) Yoon, J. H.; Ryu, D. W.; Kim, H. C.; Yoon, S. W.; Suh, B. J.; Hong, C. S. *Chem.—Eur. J.* **2009**, *15*, 3661−3665.

(22) Shen, H. Y.; Liao, D. Z.; Jiang, Z. H.; Yan, S. P.; Sun, B. W.; Wang, G. L.; Yao, X. K.; Wang, H. G. *Chem. Lett.* **1998**, 469−470.

(23) (a) Mukherjee, P.; Drew, M. G. B.; Gómez-García, C. J.; Ghosh, A. *Inorg. Chem.* **2009**, *48*, 5848−5860. (b) Ray, M. S.; Ghosh, A.; Chaudhuri, S.; Drew, M. G. B.; Ribas, J. *Eur. J. Inorg. Chem.* **2004**, 3110−3117. (c) Mukherjee, P.; Drew, M. G. B.; Estrader, M.; Ghosh., A. *Inorg. Chem.* **2008**, *47*, 7784−7791. (d) Biswas, R.; Kar, P.; Song, Y.; Ghosh, A. *Dalton Trans.* **2011**, *40*, 5324−5331.

(24) Bain, G. A.; Berry, J. F. J. *Chem. Educ.* **2008**, *85*, 532−536.

(25) CrysAlis; Oxford Diffraction Ltd.: Abingdon, U. K., 2006.

(26) Sheldrick, G. M. *Acta Crystallogr.* **2008**, *A64*, 112−122.

(27) *ABSPACK*; Oxford Diffraction Ltd: Oxford, U. K., 2005

(28) (a) Monfort, M.; Ribas, J.; Solans, X.; Font-Bardía, M. *Inorg. Chem.* **1996**, *35*, 7633−7638. (b) Ftibas, J.; Monfort, M.; Diaz, C.; Bastos, C.; Mer, C.; Solans, X. *Inorg. Chem.* **1995**, *34*, 4986−4990.

(29) Miyasaka, H.; Matsumoto, N.; Ökawa, H.; Re, N.; Gallo, E.; Floriani, C. *J. Am. Chem. Soc.* **1996**, *118*, 981−994.

(30) Sato, Y.; Miyasaka, H.; Matsumoto, N.; Ökawa, H. *Inorg. Chim. Acta* **1996**, *247*, 57−63.

(31) Fisher, M. E. *Am. J. Phys.* **1964**, *32*, 343−346.

(32) Ishii, N.; Okamura, Y.; Chiba, S.; Nogami, T.; Ishida, T. *J. Am. Chem. Soc.* **2008**, *130*, 24−25.

(33) Hibbs, W.; Rittenberg, D. K.; Sugiura, K.; Burkhart, B. M.; Morin, B. G.; Arif, A. M.; Liable-Sands, L.; Rheingold, A. L.; Sundaralingam, M.; Epstein, A. J.; Miller, J. S. *Inorg. Chem.* **2001**, *40*, 1915−1925.

(34) Mydosh, J. A. In *Spin Glasses: An Experimental Introduction*; CRC Press: Boca Raton, FL, 1993.

(35) Wang, X.; Wang, Z.; Gao, S. *Chem. Commun.* **2008**, 281−294.

(36) Mossin, S.; Weihe, H.; Osholm Sorensen, H.; Lima, N.; Sessoli, R. *Dalton Trans.* **2004**, 632−639.

(37) Sailaja, S.; Reddy, K. R.; Rajasekharan, M. V.; Hureau, C.; Riviere, E.; Cano, J.; Girerd, J. J. *Inorg. Chem.* **2003**, *42*, 180−186.

(38) Price, D. J.; Batten, S. R.; Moubaraki, B.; Murray, K. S. *Polyhedron* **2003**, *22*, 2161−2167.
(39) Palacio, F.; Andres, M.; Rodriguez-Carvajal, J.; Pannetier, J. *J. Phys.: Condens. Matter* **1991**, *3*, 2379−2390.
(40) Kennedy, B. J.; Murray, K. S. *Inorg. Chem.* **1985**, *24*, 1552−1557.
(41) Gregson, A. K.; Moxon, N. T. *Inorg. Chem.* **1982**, *21*, 586−590.
(42) Turtelli, R.; Sinnecker, J.; Triyono, D.; Grossinger, R. *J. Optoelect. Adv. Mater.* **2004**, *6*, 609−614.
(43) Marvilliers, A.; Parsons, S.; Rivière, E.; Audière, J.; Kurmoo, M.; Mallah, T. *Eur. J. Inorg. Chem.* **2001**, 1287−1293.
(44) De Jongh, L.; Miedema, A. *Adv. Phys.* **1974**, *23*, 1−260.
(45) Mitsumoto, K.; Shiga, T.; Nakano, M.; Nihei, M.; Nishikawa, H.; Oshio, H. *Eur. J. Inorg. Chem.* **2008**, 4851−4855.
(46) Bernot, K.; Luzon, J.; Sessoli, R.; Vindigni, A.; Thion, J.; Richeter, S.; Leclercq, D.; Larionova, J.; van der Lee, A. *J. Am. Chem. Soc.* **2008**, *130*, 1619−1627.